Radiology

REVIEWS AND COMMENTARY • RESEARCH IN PRACTICE

Respiratory Motion Management in Abdominal MRI: *Radiology* In Training

Pankaj Nepal, MD • Barun Bagga, MD • Li Feng, MD • Hersh Chandarana, MD, MBA

From the Department of Radiology, Massachusetts General Hospital, 55 Fruit St, Boston, MA 02114 (P.N.); Department of Radiology, New York University School of Medicine, New York, NY (B.B., H.C.); and Biomedical Engineering and Imaging Institute and Department of Radiology, Icahn School of Medicine at Mount Sinai, New York, NY (L.F.). **Address correspondence to** P.N. (email: *pankaj-123@live.com*).

Conflicts of interest are listed at the end of this article.

Radiology 2023; 306:47–53 • https://doi.org/10.1148/radiol.220448 • Content codes: GI MR

A 96-year-old woman had a suboptimal evaluation of liver observations at abdominal MRI due to significant respiratory motion. State-of-the-art strategies to minimize respiratory motion during clinical abdominal MRI are discussed.

Case Presentation (Dr Pankaj Nepal)

A 96-year-old woman with multiple comorbidities (coronary artery disease, type 2 diabetes mellitus, and severe cervical spine stenosis) presented to the emergency department with nonspecific abdominal pain and diarrhea. Contrast-enhanced CT of the abdomen and pelvis was performed to evaluate for acute abnormalities. No acute abnormalities were identified at CT, and the patient was subsequently diagnosed with *Clostridium difficile* colitis and treated appropriately. However, two indeterminate low-attenuation liver lesions were identified in segment II and segment V and/or VI, and the attenuation of both lesions was higher than that of normal fluid (Fig 1A). A dedicated contrast-enhanced MRI examination of the abdomen was performed to characterize the liver lesions. The patient was anxious, in mild distress, and claustrophobic. Although she was appropriately counseled about the importance of breath holding, the initial precontrast conventional breath-hold T1-weighted gradient-echo (GRE) images showed substantial motion artifacts (Fig 1B). A decision was made to use a commercially available gated navigator sequence for T2-weighted images (Prospective Acquisition Correction [PACE]; Siemens) (Fig 1C) and free-breathing dynamic contrast-enhanced (DCE) MRI using golden-angle radial sparse parallel (GRASP) imaging (Fig 2A–D). GRASP images showed a peripheral rim of heterogeneous late arterial phase enhancement and progressive contrast material fill-in in the portal venous and delayed phases. T2-weighted PACE images showed intermediate signal intensity in the two lesions. Delayed postcontrast conventional breath-hold T1-weighted images (Fig 2E) were also obtained after acquisition of dynamic postcontrast GRASP images (the patient was injected only once with a 6.1-mL dose of intravenous gadobutrol) but showed significant motion artifacts. Postcontrast imaging characteristics of liver lesions were better evaluated on GRASP images.

MRI findings were not diagnostic for hepatic hemangiomas because the peripheral enhancement pattern was not nodular. Typically, hemangiomas show high T2 signal intensity; however, only intermediate T2 signal intensity was present on the PACE T2-weighted images. Given the rapid enhancement (high vascularity) of the lesions, the differential diagnosis included hypervascular metastasis, cholangiocarcinoma, epithelioid hemangioendothelioma, and angiosarcoma. The patient underwent image-guided percutaneous biopsy of the segment II lesion. The histopathologic diagnosis was consistent with primary liver angiosarcoma with oligometastatic disease. Nonenhanced chest CT helped confirm the absence of distant metastasis. The patient is currently doing well 9 months after undergoing stereotactic beam radiation therapy for the right and left liver lesions.

Case Discussion (Dr Hersh Chandarana)

MRI of the abdomen faces several significant challenges owing to respiratory motion, bowel peristalsis, and the need for large volumetric coverage. Imaging is typically performed during multiple breath holds to avoid motion artifacts. The position of the upper abdominal organs, especially the liver, can vary up to several centimeters during one breathing cycle (1–3). Failed breath holding can produce substantial image blurring, resulting in degraded image quality and/or image misregistration, which may potentially mask a focal liver lesion. Herein, we aim to briefly discuss some of the methods that can be applied to manage respiratory motion in abdominal MRI.

Conventional Methods for Motion Suppression

If a patient can cooperate, breath holding, in a typical duration of 10–20 seconds, is the simplest method for avoiding respiratory motion–induced effects. This approach is currently widely used in clinical practice. Generally, because of its short repetition time and small flip angle, GRE imaging is faster than fast spin-echo or turbo spin-echo imaging. A three-dimensional (3D) T1-weighted GRE image can be obtained on the order of 10–20 seconds with parallel imaging acceleration, and images are usually acquired during suspended respiration. Multisection two-dimensional T2-weighted imaging of the whole abdomen using the turbo spin-echo sequence can take up to several minutes and can

Abbreviations

AI = artificial intelligence, CS = compressed sensing, DCE = dynamic contrast-enhanced, DL = deep learning, GRASP= golden-angle radial sparse parallel, GRE = gradient echo, MRCP = MR cholangiopancreatography, SNR = signal-to-noise ratio, 3D = three-dimensional

Summary

Several methods can be synergistically combined for motion management strategies to enable robust and diagnostic MRI of the abdomen in all patients irrespective of their breath-holding capacity.

Teaching Points

- MRI of the abdomen is frequently impaired by respiratory motion, which may potentially mask a focal lesion that would influence patient treatment.
- Several strategies can be applied to manage respiratory motion, including accelerated or free-breathing motion-robust imaging.
- Artificial intelligence methods to manage motion artifacts are under development but require testing for generalizability.

be performed in multiple breath holds, during free breathing with multiple averages, or with respiratory triggering. To shorten the breath-hold time, spatial resolution and volumetric coverage often must be sacrificed (4). With respiratory triggering or gating techniques, patients can breathe normally during an MRI examination and data can be either collected at the same phase during the respiratory cycle (triggering) or acquired continuously and then selected retrospectively (gating). This, however, significantly prolongs the overall imaging time and is not compatible with all imaging studies, such as DCE MRI (5). Such acquisition schemes may also not be reliable in patients with highly irregular breathing patterns.

Like respiratory triggering, navigator techniques prospectively coordinate specific stages of the respiratory cycle and MRI data collection by tracking the lung-liver interface with a radiofrequency pulse (6–10). Navigator echo pulses can be negatively affected by radiofrequency field distortions and can also increase radiofrequency deposition at higher magnetic field strengths, thus creating signal interference with that from the liver (3).

In our patient's case, both of these two conventional methods were deployed initially, but they still suffered from limitations. Other approaches to manage motion include *(a)* accelerated imaging that can shorten the time of image acquisition and thus a decrease in the breath-hold duration and *(b)* free-breathing image acquisition methods.

Accelerated Imaging Techniques

Accelerated or fast MRI techniques such as parallel imaging and/or compressed sensing (CS) can provide acceleration of MRI data acquisition. It should also be noted that although fast imaging alone is not a method for motion management, it can help by shortening image acquisition time and, thus, improving image quality (11) (Fig 3).

Advanced parallel imaging.—Parallel imaging is a technique that is most widely used to accelerate MRI data acquisition using arrays of receiver coils with spatially varying sensitivities (12,13). Multicoil arrays permit simultaneous encoding of MRI signals, thus allowing a reduced number of phase-encoding steps at regular intervals. The main limitation of parallel imaging is reduced signal-to-noise ratio (SNR) and severe noise amplification at high acceleration factors (>4) (14,15).

Recent advances in parallel imaging methods, such as controlled aliasing in parallel imaging results in higher acceleration (CAIPIRINHA; Siemens), enable higher acceleration. Multiple sections are excited at the same time using multiband radiofrequency pulses (16). CAIPIRINHA provides more robust parallel imaging reconstruction with fewer aliasing artifacts by optimizing the sampling mode of phase encoding. CAIPIRINHA-accelerated volumetric interpolated breath-hold examination, or VIBE, can enable further acceleration compared to standard parallel imaging, thus providing higher temporal resolution while preserving the diagnostic image quality (16–19). Time-resolved angiography with interleaved stochastic trajectories (TWIST; Siemens) is a dynamic imaging technique that combines fast volumetric 3D GRE acquisition with view-sharing reconstruction (19). Differential subsampling with Cartesian ordering (DISCO; GE Healthcare) is another rapid dynamic MRI technique that combines multiple technical features including a dual-echo spoiled gradient-echo acquisition for Dixon water-fat separation, pseudorandom variable-density k-space segmentation,

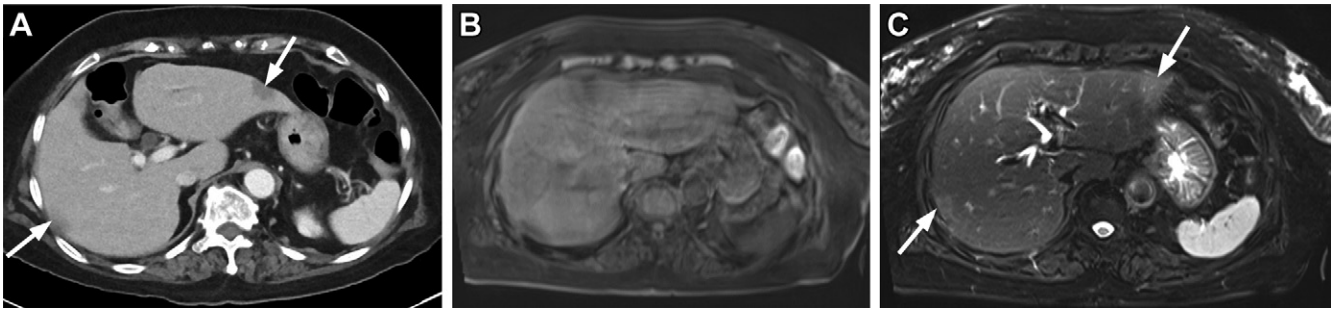

Figure 1: Images in a 96-year-old woman with acute abdominal pain. **(A)** Axial contrast-enhanced CT scan of the abdomen shows two low-attenuation lesions (arrows) in segment II of left lobe and segment V and/or VI of the right lobe of liver. **(B)** Initially acquired axial conventional breath-hold T1-weighted gradient-echo MRI scan shows avidly enhancing lesions in both lobes. Image shows significant motion artifacts, limiting accurate lesion characterization. **(C)** T2-weighted fat-saturated MRI scan acquired using a commercially available gated navigator sequence (prospective acquisition correction technique [PACE, Siemens]) helps mitigate motion artifacts and delineate the T2 intermediate character of the two lesions (arrows).

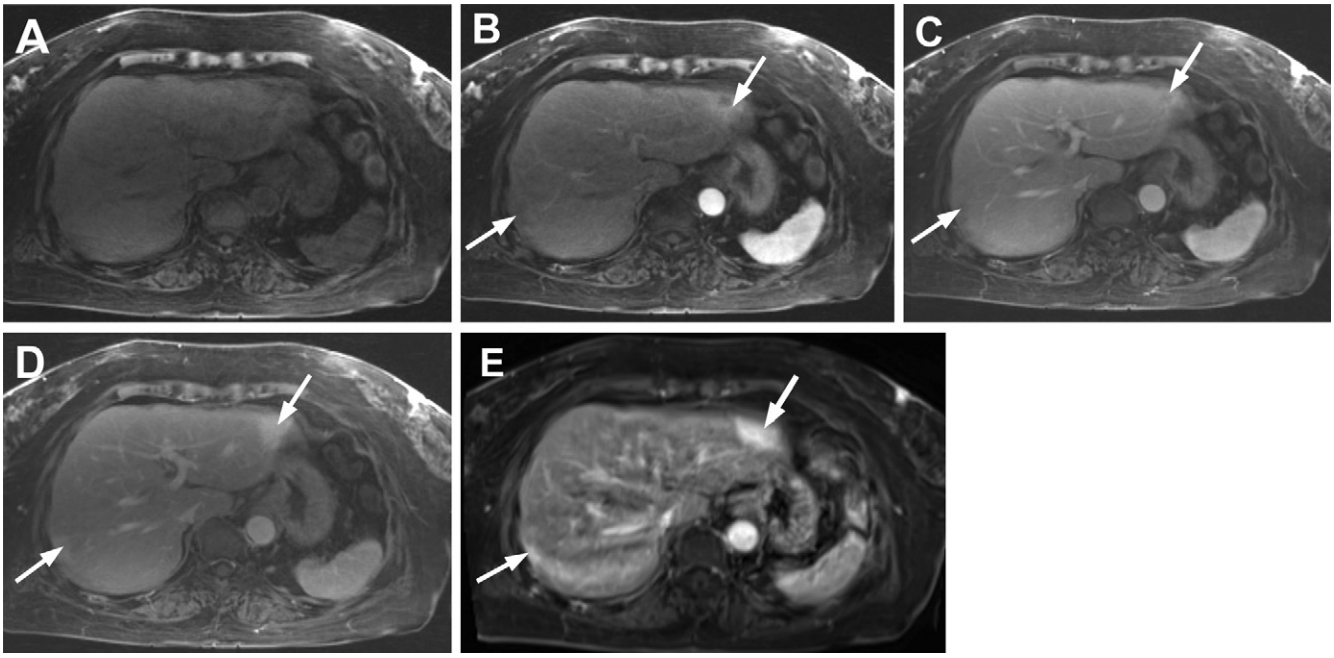

Figure 2: Axial free-breathing dynamic postcontrast images (golden-angle radial sparse parallel [GRASP]) in the same patient as in Figure 1, devoid of motion artifacts. Images obtained **(A)** before contrast material administration and **(B)** 30 seconds, **(C)** 60 seconds, and **(D)** 190 seconds after gadolinium-based contrast material administration. Contrast-enhanced images demonstrate peripheral complete rim of heterogeneous late arterial phase enhancement **(B)**, thus excluding hemangioma, with progressive centripetal contrast material fill-in on the portal venous **(C)** and delayed phase images **(D)**. **(E)** Conventional breath-hold contrast-enhanced axial T1-weighted MRI scan in delayed phase was also acquired after GRASP (the patient was injected only once with 6.1-mL dose of intravenous gadobutrol). Image shows avidly enhancing lesions in both lobes of liver. When compared to GRASP images, this breath-hold image shows significant motion artifacts limiting accurate lesion characterization. Arrows in **B**–**E** indicate lesions.

parallel imaging, and view-sharing reconstruction. It offers the advantage of achieving multiple arterial phase acquisitions during a single breath-hold period and further increases the chance of displaying arterial anatomy including small blood vessels (20).

CS method.—CS is another method that enables highly accelerated imaging by reconstructing unaliased images from undersampled measurements by exploiting the concept of image compressibility or sparsity (8). Nominal SNR is better preserved compared with parallel imaging, and it is possible to achieve higher acceleration. However, images can appear smooth if overregularized, and there is a risk of image blurring and a theoretical risk of omitting important information (8).

One example of CS in abdominal imaging includes CS 3D MR cholangiopancreatography (MRCP), which showed comparable image quality to standard 3D MRCP but with shorter imaging times (21). The use of CS enables highly accelerated 3D MRCP within a single breath hold (approximately 20 seconds), which would otherwise necessitate respiratory-triggered acquisition up to 5–6 minutes (12). CS MRCP demonstrated high diagnostic accuracy in detecting the communication between cystic lesions and the pancreatic duct (21). Combining parallel imaging with CS is also feasible in pediatric patients, with rapid image reconstruction and improved image quality devoid of motion artifacts (22).

Motion-robust MRI Acquisition

Aside from the conventional methods, newer techniques for motion-robust MRI include non-Cartesian MRI acquisition and artificial intelligence (AI)–based techniques (Table).

Different non-Cartesian MRI acquisition schemes have been shown to enable motion-robust MRI examinations, which can be performed during free breathing (23). For example, radial k-space sampling collects data along the rotating spokes that cross each other at the center of the k-space. Central k-space is repeatedly sampled in radial imaging, resulting in motion-averaged acquisition. This is an advantage over Cartesian imaging techniques in terms of motion robustness (5,24). Furthermore, with radial sampling, every spoke has a different readout direction and motion artifacts appear as mild blurring or radially oriented streaks. These streaking artifacts are more dispersed compared to Cartesian undersampling artifacts, and they could be more tolerated in clinical applications. However, it is important to note that extensive motion can still result in blurring and aliasing artifacts with radial imaging (streaks of radial trajectories) (12,13,24).

Radial imaging offers the potential for free-breathing data acquisition, but it has the disadvantage of prolonged time of image acquisition compared to Cartesian acquisition for the same acquisition parameters. Hence, additional acceleration is needed to perform dynamic imaging. One such technique for accelerated radial imaging combines CS and parallel imaging with golden angle radial sampling. GRASP imaging uses motion-robust radial acquisition in combination with CS, which allows for free-breathing acquisition (3,24). High temporal resolution can be achieved by exploiting the data sparsity presented on dynamic images. GRASP was used to perform multi-phase diagnostic imaging of the liver in our patient mentioned earlier because she could not adequately hold her breath. Theoretically, a temporal resolution of fewer than 3 seconds per volume for liver MRI is possible, but this is not necessary for clinical practice (24,25).

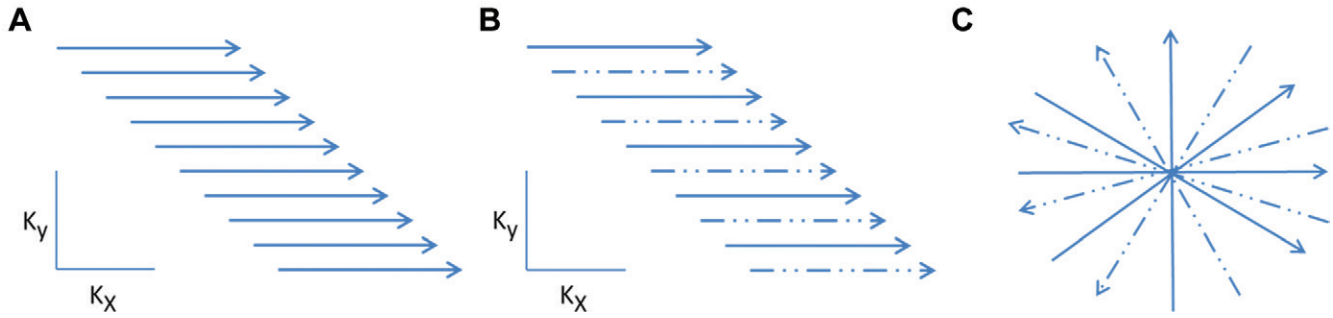

Figure 3: Diagrammatic representation of k-space acquisition. **(A)** Conventional k-space, **(B)** limited k-space (parallel or compressed sensing), and **(C)** radial imaging. Dashed lines indicate sparse sampling.

Motion-robust Acquisition Techniques

Motion Management Strategy	Advantages	Limitations
Non-Cartesian acquisition	Usually performed with radial or spiral sampling of the k-space Dense central k-space sampling results in high SNR Benefits of retrospective self-gating, no need for external device or navigator technique	Needs additional acceleration
AI-based fast imaging	Can accelerate image reconstruction, as well as improve image quality	Performance not tested widely, long training time, may be challenging to include all possible motion artifact patterns in training
AI-based artifact reduction	Wide applications, even if breath-holding ability is unpredictable	Robustness and generalizability not tested widely Needs validation

Note.—AI = artificial intelligence, SNR = signal-to-noise ratio.

Studies have shown that motion-robust free-breathing T2-weighted and contrast-enhanced T1-weighted imaging using radial sequences (T2 MultiVane XD; Philips) provide similar image quality to breath-hold sequences (25). Their application in infants and neonates resulted in a decreased need for sedation and intubation (26).

AI-based Methods for Improvement of Image Quality

AI in clinical imaging has led to breakthroughs in image classification, segmentation, super-resolution, and image reconstruction (27–30). Recently, studies have shown that AI methods can be used to remove artifacts, including residual motion artifacts, to improve image quality (29,30). Deep learning (DL) is a machine learning method that relies on neural networks with many hidden layers. A convolutional neuronal network is a DL method that has shown considerable promise in image reconstruction (30). A convolutional neuronal network can be applied either in the k-space domain to fill in the missing k-space data (before performing Fourier transform) or in the image space after performing Fourier transform to remove aliasing artifacts. Supervised training is usually performed using high-quality reference images, and the input is corresponding undersampled k-space data or images. Upon completion of the convolutional neuronal network training for a particular application, the trained neural network can be used to reconstruct new images acquired with the same undersampling pattern, allowing reduction of various streak and aliasing artifacts and substantially improving the image quality (29–33). Reconstruction of undersampled MRI data also provides opportunities for further improvement of rapid MRI (29).

AI-enabled fast imaging.—Compared with conventional rapid imaging techniques such as parallel imaging and CS, DL-based reconstruction uses a data-driven approach to characterize imaging features and removes undersampling artifacts by inferencing features from a large image database. AI-enabled accelerated T2-weighted image acquisition was performed in our second example patient (Fig 4), with approximately one-third of data collected in a single breath hold. This resulted in better image quality with reduced blurring artifacts. Image reconstruction with the DL half-Fourier acquisition single-shot turbo spin-echo sequence (HASTE; Siemens) employs a variational network composed of data consistency layers and regularizers (29). Regularizers used in DL reconstruction are data-driven, which

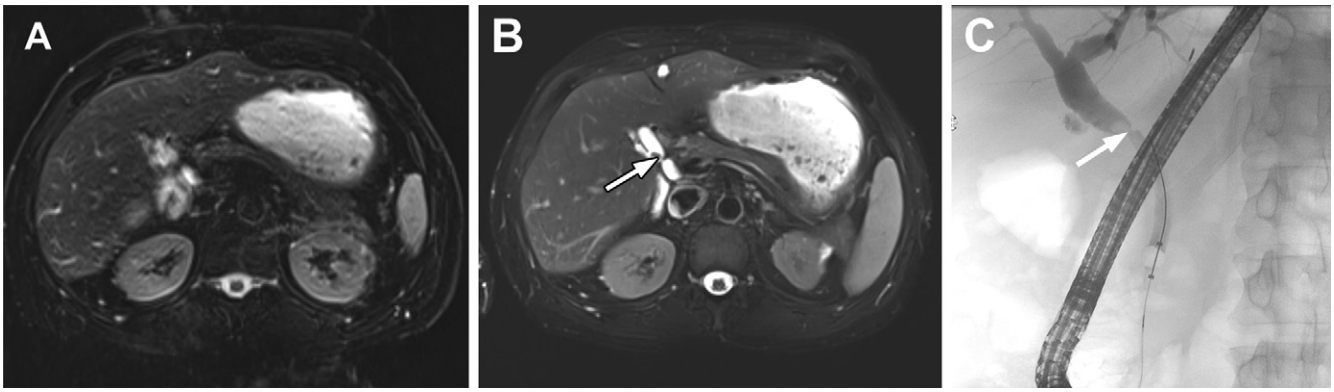

Figure 4: Images obtained after liver transplant in a 53-year-old man with a history of chronic hepatitis B and hepatocellular carcinoma. **(A)** Conventional axial T2-weighted fat-saturated MRI scan shows mild motion and phase-related artifacts causing blurring of the region of the biliary anastomoses. **(B)** Deep learning–based T2-weighted MRI scan shows significantly better anatomic clarity and reduced artifact. The accelerated image was acquired with approximately one-third of data collection in a single breath hold, resulting in better image quality with reduced blurring artifacts. Mild biliary dilatation proximal to the surgical anastomoses and a small calculus (arrow)are also clearly delineated. **(C)** Image from endoscopic retrograde cholangiopancreatography shows a filling defect at the anastomoses correlating with the calculus seen at MRI (arrow).

means they are trained specifically to reconstruct the desired type of images. These trained regularizers are possibly superior to conventional iterative reconstruction methods in denoising and correcting aliasing artifacts (30,33–36). Although DL takes a considerable amount of time for initial training, the inference is faster than conventional iterative reconstruction methods (36).

A comparison between T2-weighted MRI of the liver with DL-based image reconstruction by Shanbhogue et al (34) showed superior image quality compared to that with a conventional T2-weighted sequence despite a fourfold reduction in acquisition time. Herrmann et al (35,36) reported an acquisition time for DL-accelerated half-Fourier acquisition single-shot turbo spin-echo imaging as low as 16 seconds compared with the 4-minute acquisition time for BLADE (a proprietary name for periodically rotated overlapping parallel lines with enhanced reconstruction [PROPELLER] in MRI systems from Siemens). The acquisition time has been reduced to one or two breath holds, with a reduction in respiratory motion and ghosting artifacts, and increased lesion conspicuity (37). Our second patient example with DL-accelerated half-Fourier acquisition single-shot turbo spin-echo (Fig 4) was evaluated with a 3-T MRI scanner with a single breath-hold acquisition and 55 seconds of overall acquisition time (including instructions for breath holding plus a single breath-hold acquisition), with a postprocessing time of 5 minutes. This is a research sequence that is added to our liver protocol with certain scanners. DL reconstruction has also been evaluated for turbo spin-echo acquisition of the abdominopelvic organs. For example, DL turbo spin-echo imaging of the prostate allowed a two-thirds reduction of examination time yet improved image quality, lesion detection, and diagnostic confidence (38).

AI-enabled DCE MRI.—DCE MRI requires an accelerated acquisition of data to achieve high spatiotemporal resolution. A compromise on the spatial resolution has an adverse effect on the evaluation of morphologic characteristics, whereas poor temporal resolution has a negative effect on the analysis of tissue perfusion. Unfortunately, these two requirements are in direct conflict. Various acquisition and reconstruction methods with parallel imaging or CS have been used to accelerate DCE MRI (35–40). Conventional CS-based reconstruction techniques usually suffer from long computational times, and their performance depends on the choice of the sparsity constraint (39). Various AI-enabled techniques such as deep neural networks learn the reconstruction process from existing data sets (during training), thus providing a fast and efficient reconstruction that can be applied to newly acquired data (39,40).

AI-enabled artifact reduction.—U-Net is a widely accepted algorithm that uses a multiresolution convolutional network for the segmentation, reconstruction, and denoising of MRI scans (41–44). Most of the artifacts observed on MRI scans, such as motion, aliasing, or streak artifacts, are distributed globally on the image domain. U-Net uses a large receptive field, and these artifacts can be effectively removed using global structural information (41–44). Advanced DL methods, such as generative adversarial networks, comprise two networks called the generator and discriminator. U-Net enables both rigid as well as nonrigid motion correction (43). A method for respiratory motion correction was proposed by Jiang et al (45) using a generative adversarial network–based network with a U-Net generator. A denoising filter known as motion artifact reduction method based on convolutional neural network (MARC) has been used for DCE MRI of the liver. MARC employs convolution operations between input and output filters, therefore successfully extracting the motion artifacts and blurring without affecting the contrast-to-noise ratio and SNR of the images (31).

Currently, the major goal of AI is to improve the robustness of DL-based image reconstruction against discrepancies in undersampling schemes that may occur between training and inference (30–32). DL-based reconstruction could benefit from extensively varying undersampling patterns during the training

process, leading to better generalization and performance of the trained network in the removal of undersampling artifacts. SANTIS (sampling-augmented neural network with incoherent structure) is one such method for robust MRI reconstruction. SANTIS has been used for artifact reduction in radial-based imaging of the liver (32).

Several DL techniques have been used to reduce artifacts at postprocessing (45,46). The application of a DL-based denoising approach to MRCP images resulted in a reduction of motion artifacts, higher SNR, improved duct visibility, and improved overall image quality (45). DL-based super-resolution reconstruction, a postprocessing technique, combines multiple low-resolution two-dimensional image stacks into a single high-resolution 3D visualization, enhancing sharpness and lesion conspicuity in the liver and on MRCP images (47).

Challenges with AI Techniques

One of the challenges for various DL techniques is their generalizability. It remains to be studied what the performance of these methods will be when these methods are applied to data that were not included in the initial training (eg, from a different scanner and patient population). DL techniques also need validation in terms of diagnostic performance in a larger patient cohort, hopefully in multi-center trials. There is a growing body of literature documenting the artifacts introduced by DL methods, for instance band or streaking artifacts, or DL reconstruction instabilities (48,49). Tiny alterations in both image as well as sampling domain can lead to a myriad of different artifacts, which can be unpredictable for different trained networks. Failure of recovering structural changes on the reconstructed images may lead to masking of small lesions, introduction of pseudolesions, or distortions and blurring of the imaging features (48). DL reconstruction instabilities are not necessarily rare events, and a future challenge may be finding effective remedies.

Conclusion

In summary, we have briefly discussed various methods to overcome motion-related challenges in abdominopelvic MRI. These include methods for accelerated imaging such as advanced parallel imaging, CS, and DL-based methods as well as free-breathing methods such as non-Cartesian imaging. The methods can be synergistically combined for improved management of respiratory motion. For example, motion-robust acquisition can be combined with acceleration methods to improve imaging performance compared to either of them alone. In addition, AI-based methods can be combined with other motion management strategies to enable robust and diagnostic imaging of the abdomen in all patients irrespective of their breath-holding capacity.

Acknowledgment: We acknowledge our patients.

Disclosures of conflicts of interest: P.N. No relevant relationships. **B.B.** No relevant relationships. **L.F.** Support from NIH grants R01EB030549 and R01EB031083; patent on GRASP and XD-GRASP techniques. **H.C.** Patent on GRASP and XD-GRASP techniques; research support in the form of hardware from Siemens Healthcare as part of Master Research Agreement.

References

1. Schultz CL, Alfidi RJ, Nelson AD, Kopiwoda SY, Clampitt ME. The effect of motion on two-dimensional Fourier transformation magnetic resonance images. Radiology 1984;152(1):117–121.
2. Axel L, Summers RM, Kressel HY, Charles C. Respiratory effects in two-dimensional Fourier transform MR imaging. Radiology 1986;160(3):795–801.
3. Feng L, Axel L, Chandarana H, Block KT, Sodickson DK, Otazo R. XD-GRASP: Golden-angle radial MRI with reconstruction of extra motion-state dimensions using compressed sensing. Magn Reson Med 2016;75(2):775–788.
4. Paling MR, Brookeman JR. Respiration artifacts in MR imaging: reduction by breath holding. J Comput Assist Tomogr 1986;10(6):1080–1082.
5. Chandarana H, Block TK, Rosenkrantz AB, et al. Free-breathing radial 3D fat-suppressed T1-weighted gradient echo sequence: a viable alternative for contrast-enhanced liver imaging in patients unable to suspend respiration. Invest Radiol 2011;46(10):648–653.
6. Stuber M, Botnar RM, Fischer SE, et al. Preliminary report on in vivo coronary MRA at 3 Tesla in humans. Magn Reson Med 2002;48(3):425–429.
7. Jiang W, Ong F, Johnson KM, et al. Motion robust high resolution 3D free-breathing pulmonary MRI using dynamic 3D image self-navigator. Magn Reson Med 2018;79(6):2954–2967.
8. Feng L, Benkert T, Block KT, Sodickson DK, Otazo R, Chandarana H. Compressed sensing for body MRI. J Magn Reson Imaging 2017;45(4):966–987.
9. Bydder M, Larkman DJ, Hajnal JV. Detection and elimination of motion artifacts by regeneration of k-space. Magn Reson Med 2002;47(4):677–686.
10. Uribe S, Muthurangu V, Boubertakh R, et al. Whole-heart cine MRI using real-time respiratory self-gating. Magn Reson Med 2007;57(3):606–613.
11 Schreiber-Zinaman J, Rosenkrantz AB. Frequency and reasons for extra sequences in clinical abdominal MRI examinations. Abdom Radiol (NY) 2017;42(1):306–311.
12. Yoon JH, Nickel MD, Peeters JM, Lee JM. Rapid Imaging: Recent Advances in Abdominal MRI for Reducing Acquisition Time and Its Clinical Applications. Korean J Radiol 2019;20(12):1597–1615.
13. Budjan J, Schoenberg SO, Riffel P. Fast Abdominal Magnetic Resonance Imaging. Rofo 2016;188(6):551–558.
14. Recht MP, Zbontar J, Sodickson DK, et al. Using Deep Learning to Accelerate Knee MRI at 3 T: Results of an Interchangeability Study. AJR Am J Roentgenol 2020;215(6):1421–1429.
15. Yang RK, Roth CG, Ward RJ, deJesus JO, Mitchell DG. Optimizing abdominal MR imaging: approaches to common problems. RadioGraphics 2010;30(1):185–199.
16. Hu J, Xu B, Cao J, et al. Application value of CAIPIRINHA-VIBE with MOCO in liver magnetic resonance examination. Eur J Radiol 2021;140:109739.
17. Erol MY, Algin O. Detection of intramural fat accumulation by 3D-Dixon-Caipirinha-Vibe and the contribution of this technique to the determination of the chronicity of Chron's disease. Magn Reson Imaging 2022;85:93–101.
18. Othman AE, Martirosian P, Schraml C, et al. Feasibility of CAIPIRINHA-Dixon-TWIST-VIBE for dynamic contrast-enhanced MRI of the prostate. Eur J Radiol 2015;84(11):2110–2116.
19. Kazmierczak PM, Theisen D, Thierfelder KM, et al. Improved detection of hypervascular liver lesions with CAIPIRINHA-Dixon-TWIST-volume-interpolated breath-hold examination. Invest Radiol 2015;50(3):153–160.
20. Wei Y, Chen G, Tang H, et al. Improved Display of Hepatic Arterial Anatomy Using Differential Subsampling With Cartesian Ordering (DISCO) With Gadoxetic Acid-Enhanced MRI: Comparison With Single Arterial Phase MRI and Computed Tomographic Angiography. J Magn Reson Imaging 2020;51(6):1766–1776.
21. He M, Xu J, Wu Q, et al. Application of Compressed Sensing 3D MR cholangiopancreatography (CS-MRCP) with Contact-Free Physiological Monitoring (CFPM) for Pancreaticobiliary Disorders. Acad Radiol 2021;28(Suppl 1):S148–S156.
22. Zhang T, Chowdhury S, Lustig M, et al. Clinical performance of contrast enhanced abdominal pediatric MRI with fast combined parallel imaging compressed sensing reconstruction. J Magn Reson Imaging 2014;40(1):13–25.
23. Yoon JH, Lee JM, Yu MH, et al. Evaluation of Transient Motion During Gadoxetic Acid-Enhanced Multiphasic Liver Magnetic Resonance Imaging Using Free-Breathing Golden-Angle Radial Sparse Parallel Magnetic Resonance Imaging. Invest Radiol 2018;53(1):52–61.

24. Feng L. Golden-Angle Radial MRI: Basics, Advances, and Applications. J Magn Reson Imaging. 2022 Apr 9. doi: 10.1002/jmri.28187. Epub ahead of print.
25. Sodhi KS, Bhatia A, Lee EY. Prospective Evaluation of Free-Breathing Fast T2-Weighted MultiVane XD Sequence at 3-T MRI for Large Airway Assessment in Pediatric Patients. AJR Am J Roentgenol 2021;216(4):1074–1080.
26. Sandino CM, Cheng JY, Chen F, Mardani M, Pauly JM, Vasanawala SS. Compressed Sensing: From Research to Clinical Practice with Deep Neural Networks. IEEE Signal Process Mag 2020;37(1):111–127.
27. Knoll F, Hammernik K, Zhang C, et al. Deep-Learning Methods for Parallel Magnetic Resonance Imaging Reconstruction: A Survey of the Current Approaches, Trends, and Issues. IEEE Signal Process Mag 2020;37(1):128–140.
28. Chen F, Taviani V, Malkiel I, et al. Variable-Density Single-Shot Fast Spin-Echo MRI with Deep Learning Reconstruction by Using Variational Networks. Radiology 2018;289(2):366–373.
29. Kozak BM, Jaimes C, Kirsch J, Gee MS. MRI Techniques to Decrease Imaging Times in Children. RadioGraphics 2020;40(2):485–502.
30. Zucker EJ, Sandino CM, Kino A, Lai P, Vasanawala SS. Free-breathing Accelerated Cardiac MRI Using Deep Learning: Validation in Children and Young Adults. Radiology 2021;300(3):539–548.
31. Tamada D, Kromrey ML, Ichikawa S, Onishi H, Motosugi U. Motion Artifact Reduction Using a Convolutional Neural Network for Dynamic Contrast Enhanced MR Imaging of the Liver. Magn Reson Med Sci 2020;19(1):64–76.
32. Liu F, Samsonov A, Chen L, Kijowski R, Feng L. SANTIS: Sampling-Augmented Neural neTwork with Incoherent Structure for MR image reconstruction. Magn Reson Med 2019;82(5):1890–1904.
33. Kromrey ML, Tamada D, Johno H, et al. Reduction of respiratory motion artifacts in gadoxetate-enhanced MR with a deep learning-based filter using convolutional neural network. Eur Radiol 2020;30(11):5923–5932.
34. Shanbhogue K, Tong A, Smereka P, et al. Accelerated single-shot T2-weighted fat-suppressed (FS) MRI of the liver with deep learning-based image reconstruction: qualitative and quantitative comparison of image quality with conventional T2-weighted FS sequence. Eur Radiol 2021;31(11):8447–8457.
35. Herrmann J, Gassenmaier S, Nickel D, et al. Diagnostic Confidence and Feasibility of a Deep Learning Accelerated HASTE Sequence of the Abdomen in a Single Breath-Hold. Invest Radiol 2021;56(5):313–319.
36. Herrmann J, Nickel D, Mugler JP 3rd, et al. Development and Evaluation of Deep Learning-Accelerated Single-Breath-Hold Abdominal HASTE at 3 T Using Variable Refocusing Flip Angles. Invest Radiol 2021;56(10):645–652.
37. Knoll F, Zbontar J, Sriram A, et al. fastMRI: A Publicly Available Raw k-Space and DICOM Dataset of Knee Images for Accelerated MR Image Reconstruction Using Machine Learning. Radiol Artif Intell 2020;2(1):e190007.
38. Gassenmaier S, Afat S, Nickel D, Mostapha M, Herrmann J, Othman AE. Deep learning-accelerated T2-weighted imaging of the prostate: Reduction of acquisition time and improvement of image quality. Eur J Radiol 2021;137:109600.
39. Bustin A, Fuin N, Botnar RM, Prieto C. From Compressed-Sensing to Artificial Intelligence-Based Cardiac MRI Reconstruction. Front Cardiovasc Med 2020;7:17.
40. Browne LP, Malone LJ, Englund EK, et al. Free-breathing magnetic resonance imaging with radial k-space sampling for neonates and infants to reduce anesthesia. Pediatr Radiol 2022. 10.1007/s00247-022-05298-7. Published online February 16, 2022.
41. Lee D, Yoo J, Tak S, Ye JC. Deep Residual Learning for Accelerated MRI Using Magnitude and Phase Networks. IEEE Trans Biomed Eng 2018;65(9):1985–1995.
42. Yang G, Yu S, Dong H, et al. DAGAN: Deep De-Aliasing Generative Adversarial Networks for Fast Compressed Sensing MRI Reconstruction. IEEE Trans Med Imaging 2018;37(6):1310–1321.
43. Hyun CM, Kim HP, Lee SM, Lee S, Seo JK. Deep learning for undersampled MRI reconstruction. Phys Med Biol 2018;63(13):135007.
44. Dalmış MU, Litjens G, Holland K, et al. Using deep learning to segment breast and fibroglandular tissue in MRI volumes. Med Phys 2017;44(2):533–546.
45. Jiang W, Liu Z, Lee KH, et al. Respiratory motion correction in abdominal MRI using a densely connected U-Net with GAN-guided training. arXiv:1906.09745 [preprint]. https://arxiv.org/ftp/arxiv/papers/1906/1906.09745.pdf. Posted June 24, 2019.
46. Jaubert O, Montalt-Tordera J, Knight D, et al. Real-time deep artifact suppression using recurrent U-Nets for low-latency cardiac MRI. Magn Reson Med 2021;86(4):1904–1916.
47. Ebner M, Patel PA, Atkinson D, et al. Super-resolution for upper abdominal MRI: Acquisition and post-processing protocol optimization using brain MRI control data and expert reader validation. Magn Reson Med 2019;82(5):1905–1919.
48. Antun V, Renna F, Poon C, Adcock B, Hansen AC. On instabilities of deep learning in image reconstruction and the potential costs of AI. Proc Natl Acad Sci U S A 2020;117(48):30088–30095.
49. Hyun CM, Baek SH, Lee M, Lee SM, Seo JK. Deep learning-based solvability of underdetermined inverse problems in medical imaging. Med Image Anal 2021;69:101967.

Pankaj Nepal, MD, is an abdominal imaging fellow at Massachusetts General Hospital, Boston. He has received many awards from RSNA and AUR. His major interest is in advanced applications of abdominal MRI.

Hersh Chandarana, MD, MBA, is a professor of radiology and urology and associate chair for clinical and translational research in the Department of Radiology at NYU Langone Health. He is a clinician scientist with research interest in development of novel imaging methods for oncologic and functional imaging.